SUPPLEMENTAL FIGURES

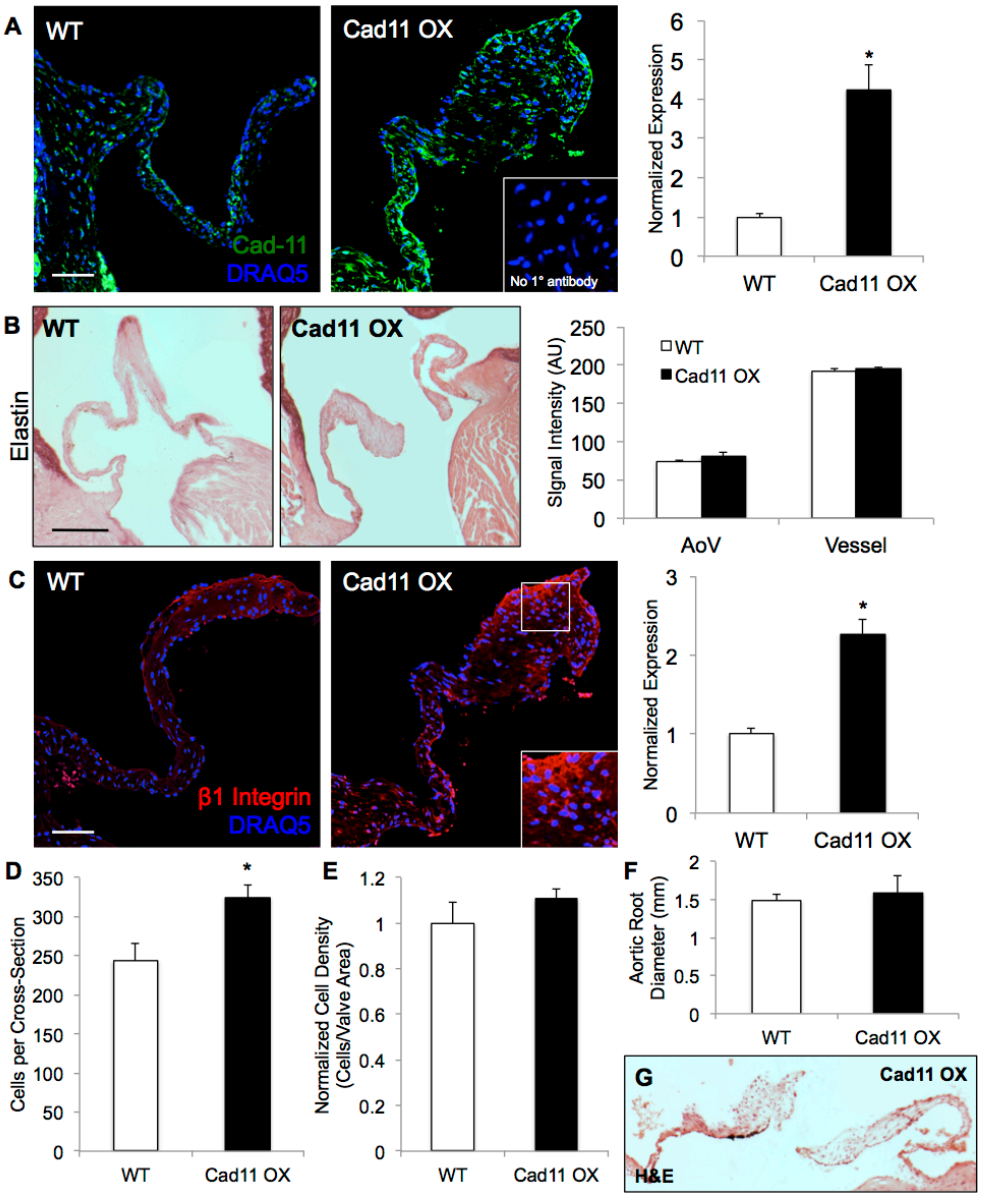

Figure SI. A, Immunohistochemistry confirms Cad-11 overexpression in mouse aortic valves in Cad11 OX mice compared to WT at 10 months (n=5, *p<0.01), and sections treated with no primary antibody display minimal non-specific staining (insert) Scale bar=50μm. **B,** Cad11 OX AoVs display equal elastin compared to WT mice at 10 months (n=6) Scale bar=50μm. **C,** Cad11 OX AoV have greater β1 integrin expression compared to WT mice at 10 months (n=4) Scale bar=200μm. **D,E,** Cad11 OX mice have significantly more number of cells in a cross-section, but have equal cell density compared to WT controls at 10 months (n=8, *p<0.0005). **F,** WT and Cad11 OX mice do not differ in aortic root diameter at 10 months as measured by echocardiography (n=5). **G,** H&E staining shows minimal artifact staining. Significance was determined using the Student's t-test.

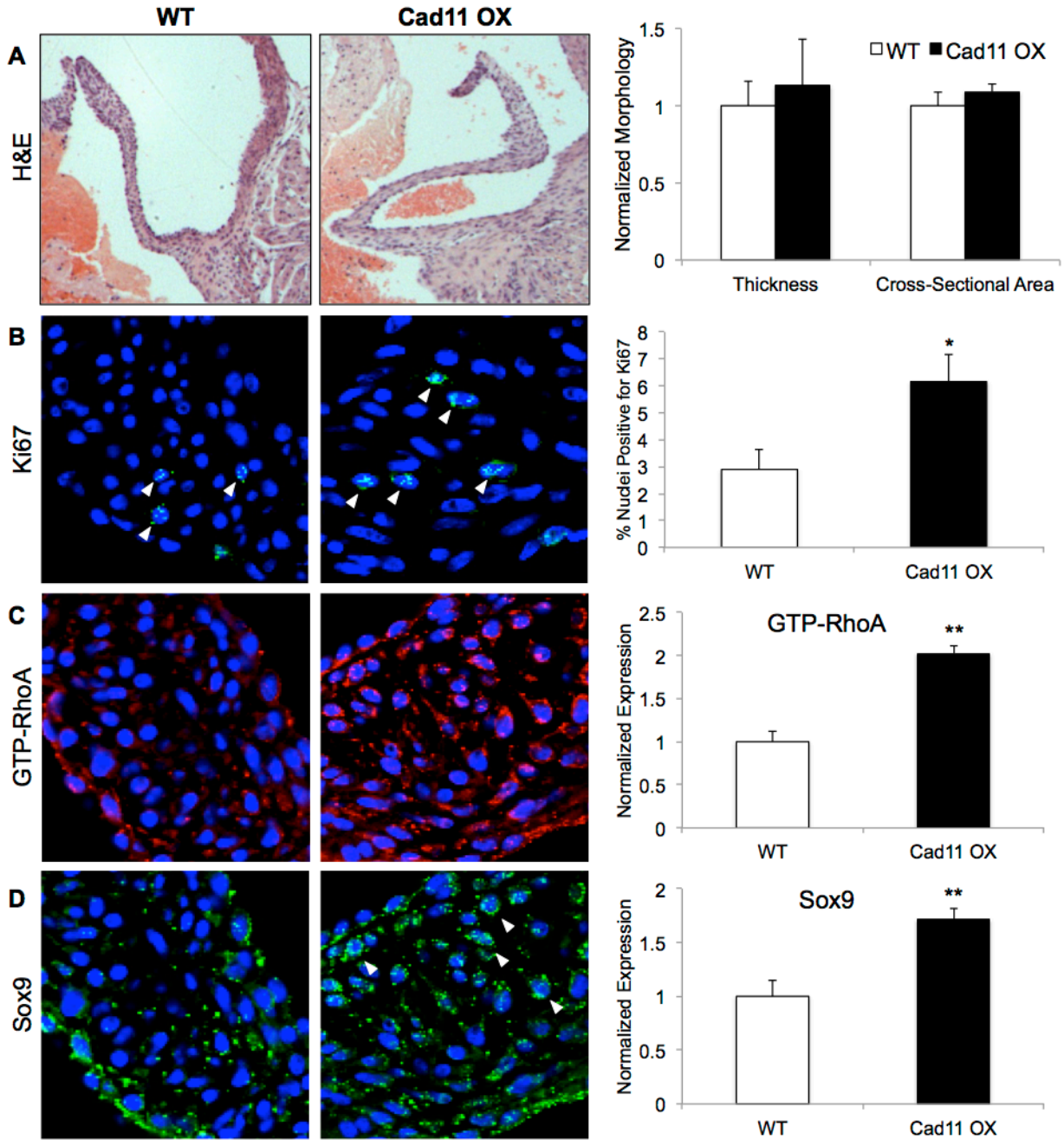

Figure SII. A, At 1 month, WT and Cad11 OX mice do not differ significantly in aortic valve morphology as measured by valve thickness and cross-sectional area. **B,** Cad11 OX AoVs have more Ki67 positive cells than WT mice at 1 month, indicating increased proliferation. **C,D,** Cad11 OX AoVs display increased GTP-RhoA and Sox9 activity relative to WT mice at 1 month. White arrows indicate Sox9 localized to the nucleus. Significance was determined using the Student's t-test (n=4, *p<0.05, **p<0.001).

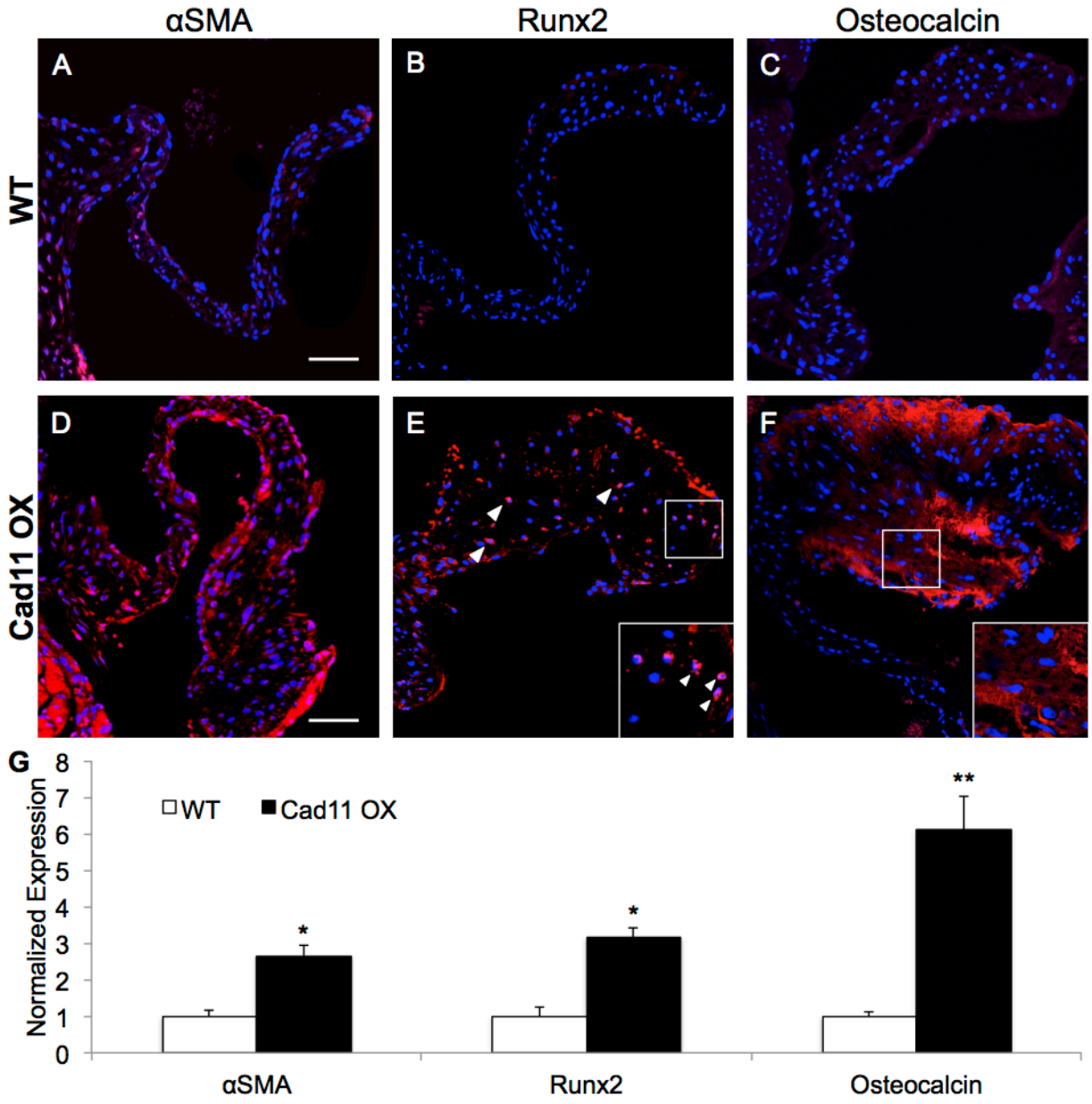

Figure SIII. Increased αSMA indicate an activated, myofibroblastic phenotype in diseased Cad11 OX AoVs compared to WT at 10 months (**A,D**). Cad11 OX mice highly express markers of osteoblastic differentiation Runx2 (white arrowheads) and Osteocalcin at 10 months whereas expression is limited in WT mice (**B,C,E,F**). Significance was determined using the Student's t-test (αSMA n≥4, Runx2 n=3, Osteocalcin n≥5, *p<0.005, **p<0.001) Scale bar=50μm

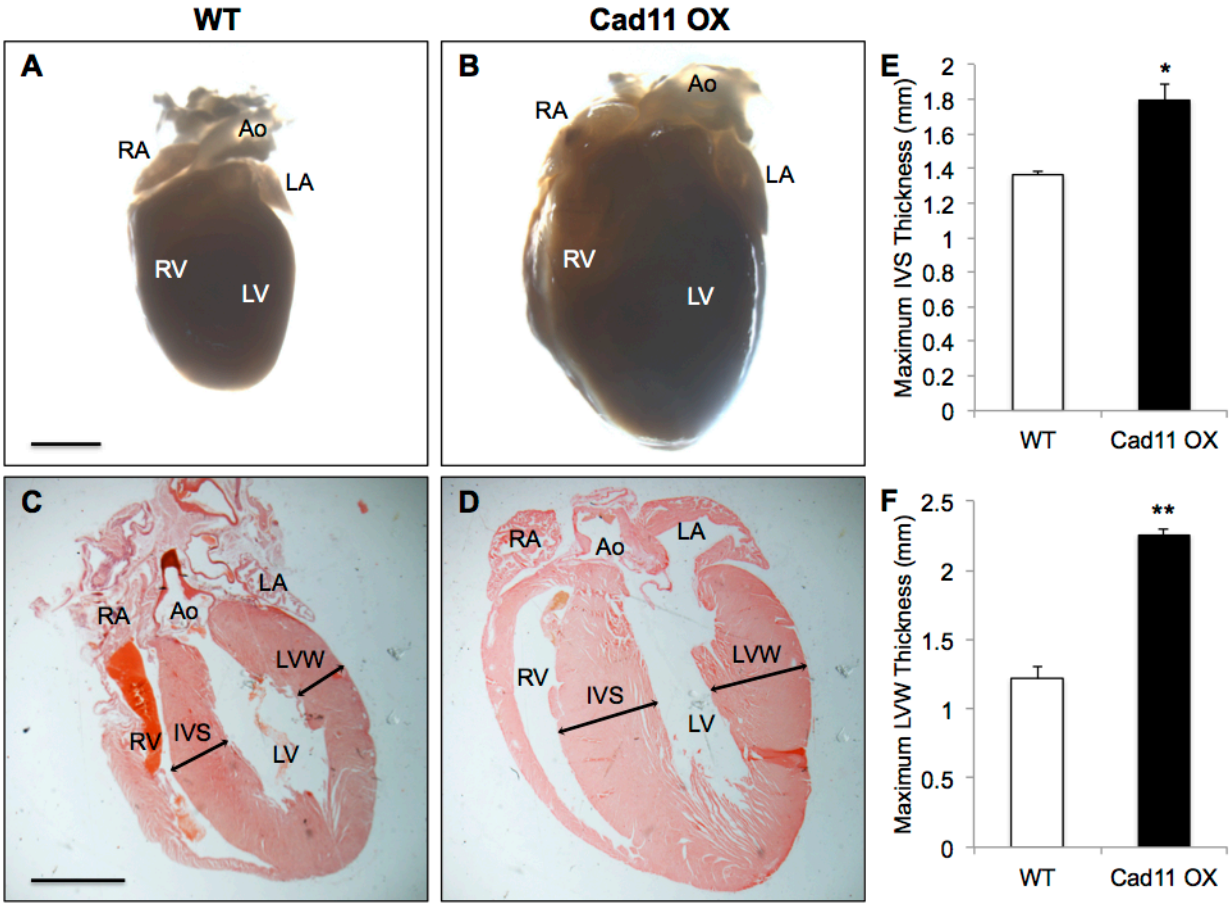

Figure SIV. Cad11 OX mice have larger hearts compared to WT controls at 10 months (**A,B**) due to left ventricular hypertrophy with thickening of the interventricular septum and left ventricular wall as indicated by H&E staining (**C-F**). Significance was determined using the Student's t-test (n=6, *p<0.005 **p<2E-5). Scale bars=2mm (Ao=aorta; LA=left atrium; LV=left ventricle; RA=right atrium; RV=right ventricle; IVS=interventricular septum; LVW=left ventricular wall).

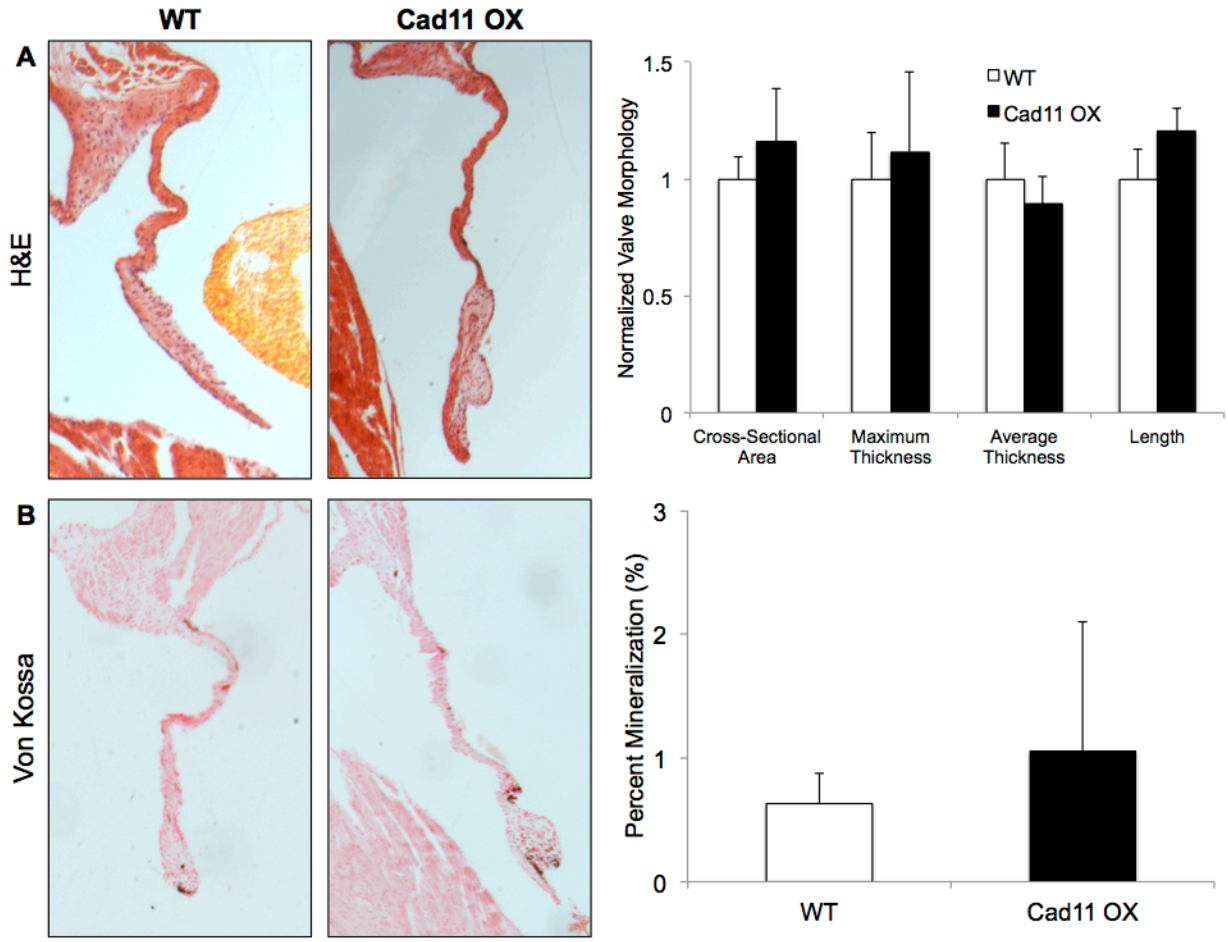

Figure SV. A, Cad11 OX and WT mice do not differ significantly in mitral valve morphology as measured by valve cross-sectional area, maximum valve thickness, average valve thickness, and valve length at 10 months (n=4). **B,** Von Kossa staining reveals that WT and Cad11 OX mice do not differ in mitral valve mineralization at 10 months (n=4). Significance was determined using the Student's t-test at $p<0.05$.

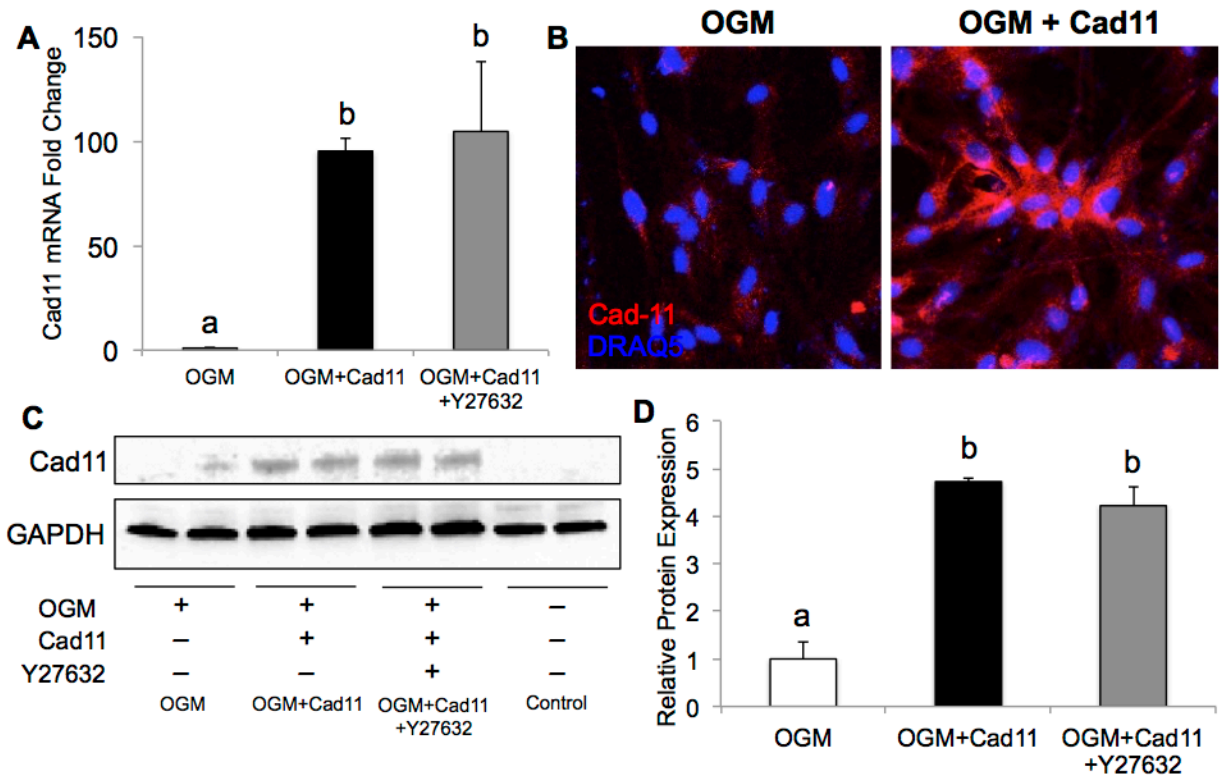

Figure SVI. A, qRT-PCR demonstrates a ~100 fold increase in Cad-11 mRNA following transfection with the Cad-11 plasmid. Bars that do not share any letters are significantly different according to a one-way ANOVA with Tukey's post-hoc test ($p<0.05$, $n=4$). **B,** Immunohistochemistry qualitatively shows an increase in Cad11 (red) at the protein level. **C,D,** Western blotting quantitatively shows an increase in Cad-11 protein expression relative to control plasmid in OGM. Bars that do not share any letters are significantly different according to a one-way ANOVA with Tukey's post-hoc test ($p<0.05$, $n=4$).

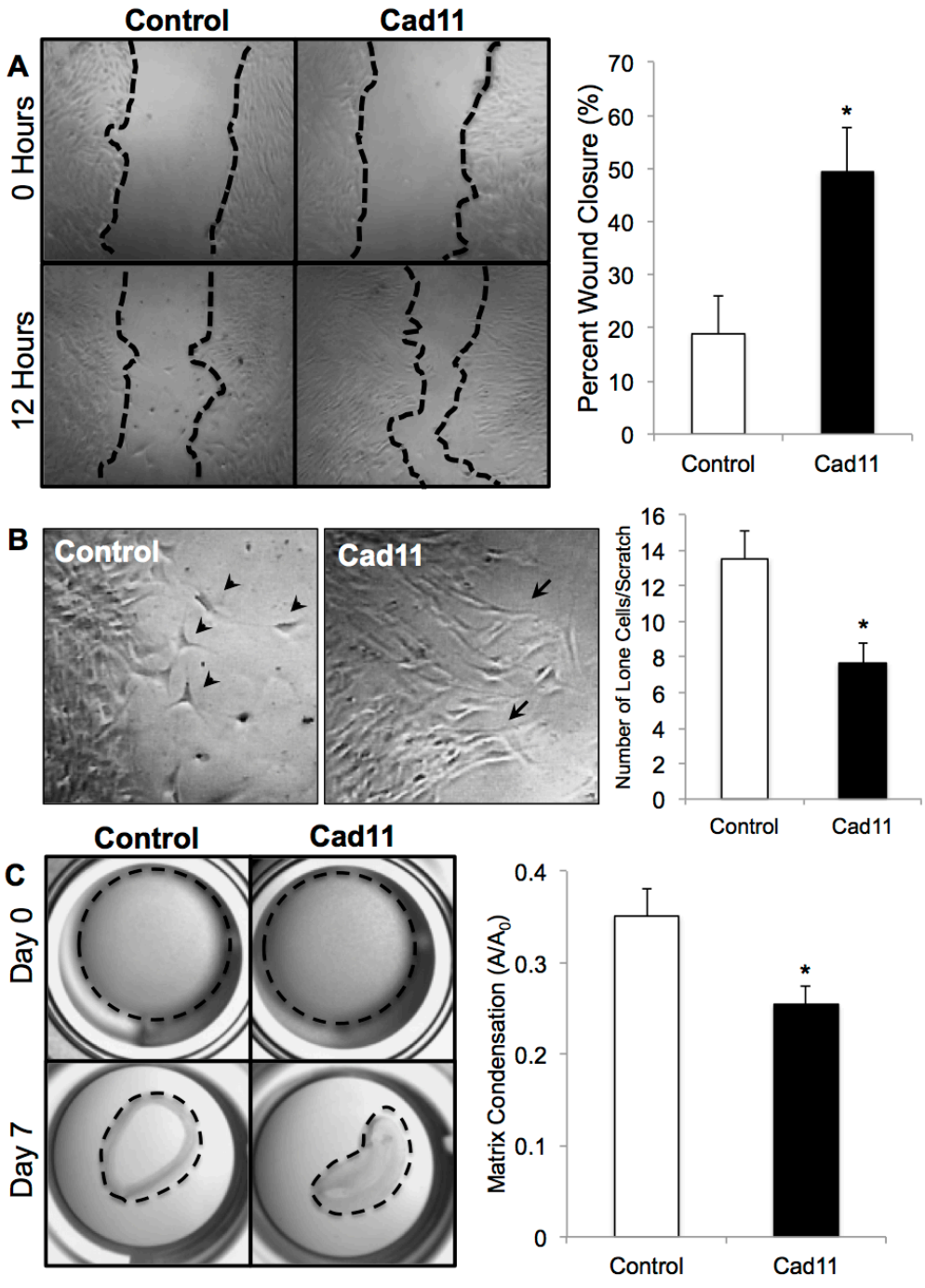

Figure SVII. A, PAVICs transfected with a Cad-11 overexpressing plasmid exhibit increased migration compared to control cells in a wound closure assay after 12 hours (n=6, *p<0.05). **B,** Quantification of number of lone cells (<4 in-contact neighboring cells) reveals that control PAVICs have more lone, migrating cells than Cad-11 transfected PAVICs, which migrate mostly as a collective front (n=7, *p<0.01). **C,** Cad-11 overexpressing PAVICs displayed greater compaction in a free-floating 3D collagen gel compared to control cells after 7 days (n=6, *p<0.05). Significance was determined using the Student's t-test at p<0.05.

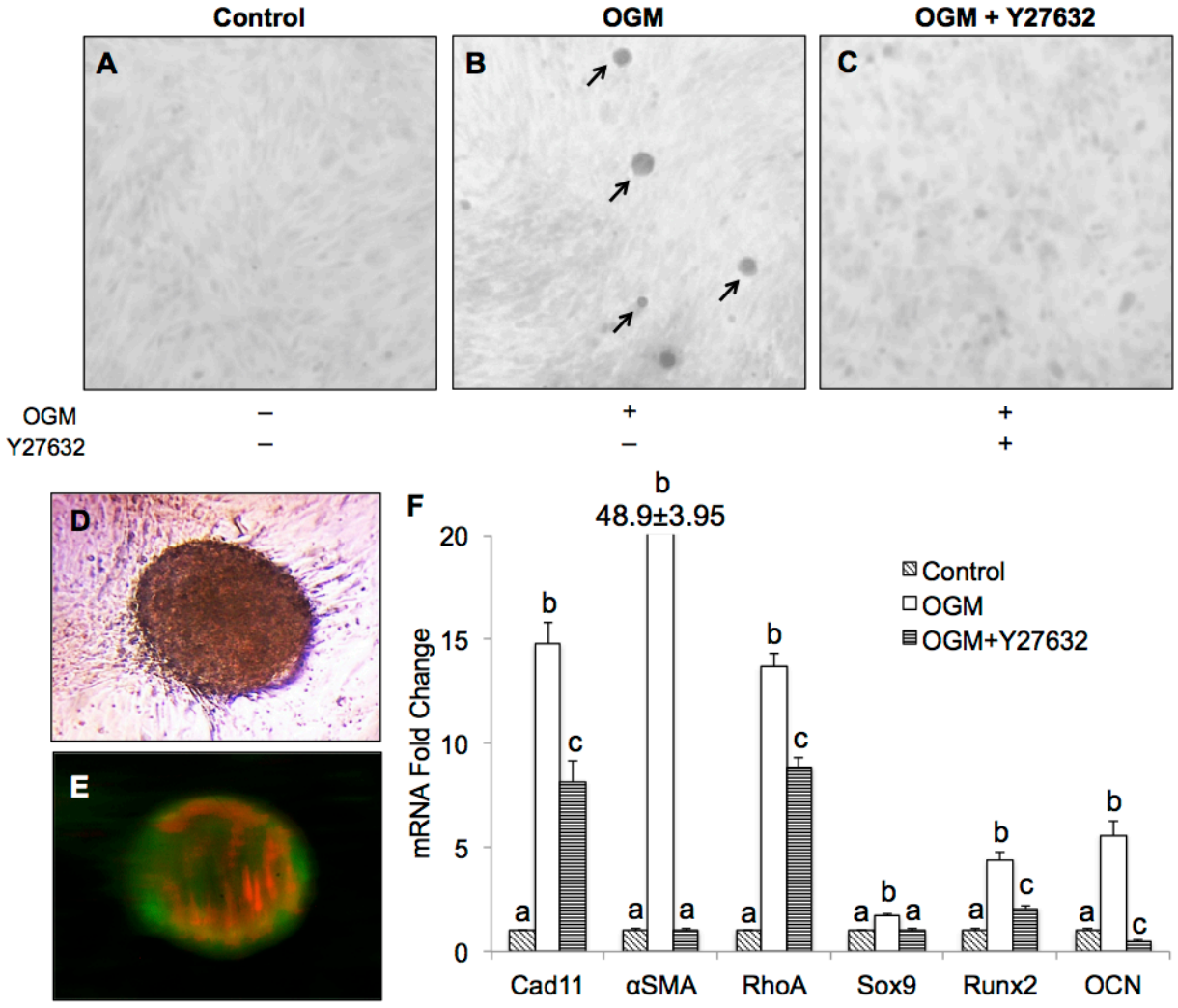

Figure SVIII. At 10 days, PAVICs in regular growth media (**A**) do not calcify, while cells in OGM (**B**) form multiple Alizarin Red-positive calcific nodules. Treatment with Y27632 (**C**) prevents nodule formation. **D,** Brightfield imaging of calcific nodules shows aggregation of cells. **E,** Live/Dead staining shows the nodules have a partially apoptotic core. **F,** Quantitative real-time PCR shows differences in gene expression among PAVICs in the three conditions relative to control Bars that do not share any letters are significantly different according to a one-way ANOVA with Tukey's post-hoc test ($p<0.01$, $n=4$).

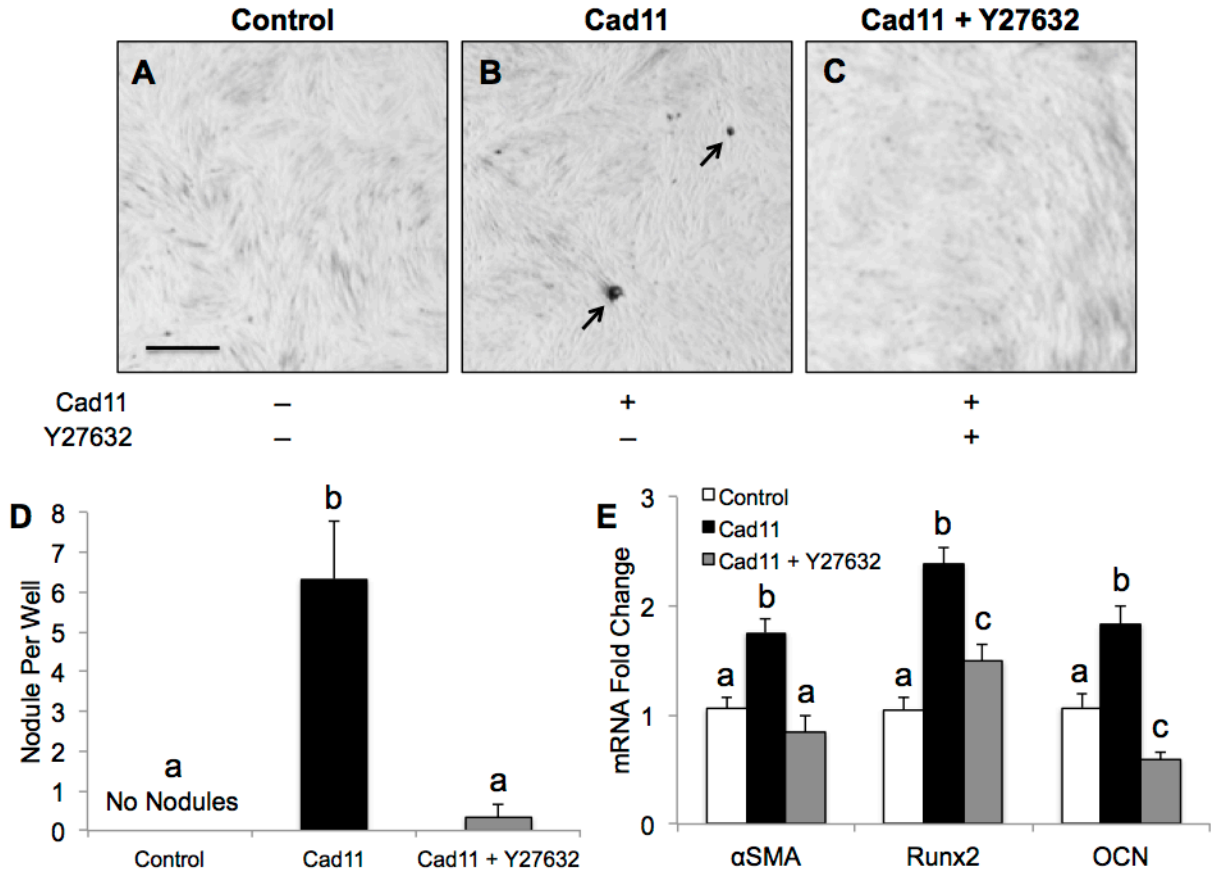

Figure SIX. At 10 days, PAVICs in regular growth media (**A**) do not calcify, while Cad-11 overexpressing cells (**B**) form small, Alizarin Red-positive calcific nodules (arrows). Treatment with Y27632 (**C**) prevents nodule formation. **D,** Quantification of calcific nodules per well. Bars that do not share any letters are significantly different according to a one-way ANOVA with Tukey's post-hoc test ($p<0.05$, $n=4$). **E,** qRT-PCR shows differences in gene expression among PAVICs in the three conditions compared to control. Bars that do not share any letters are significantly different according to a one-way ANOVA with Tukey's post-hoc test ($p<0.01$, $n=4$).

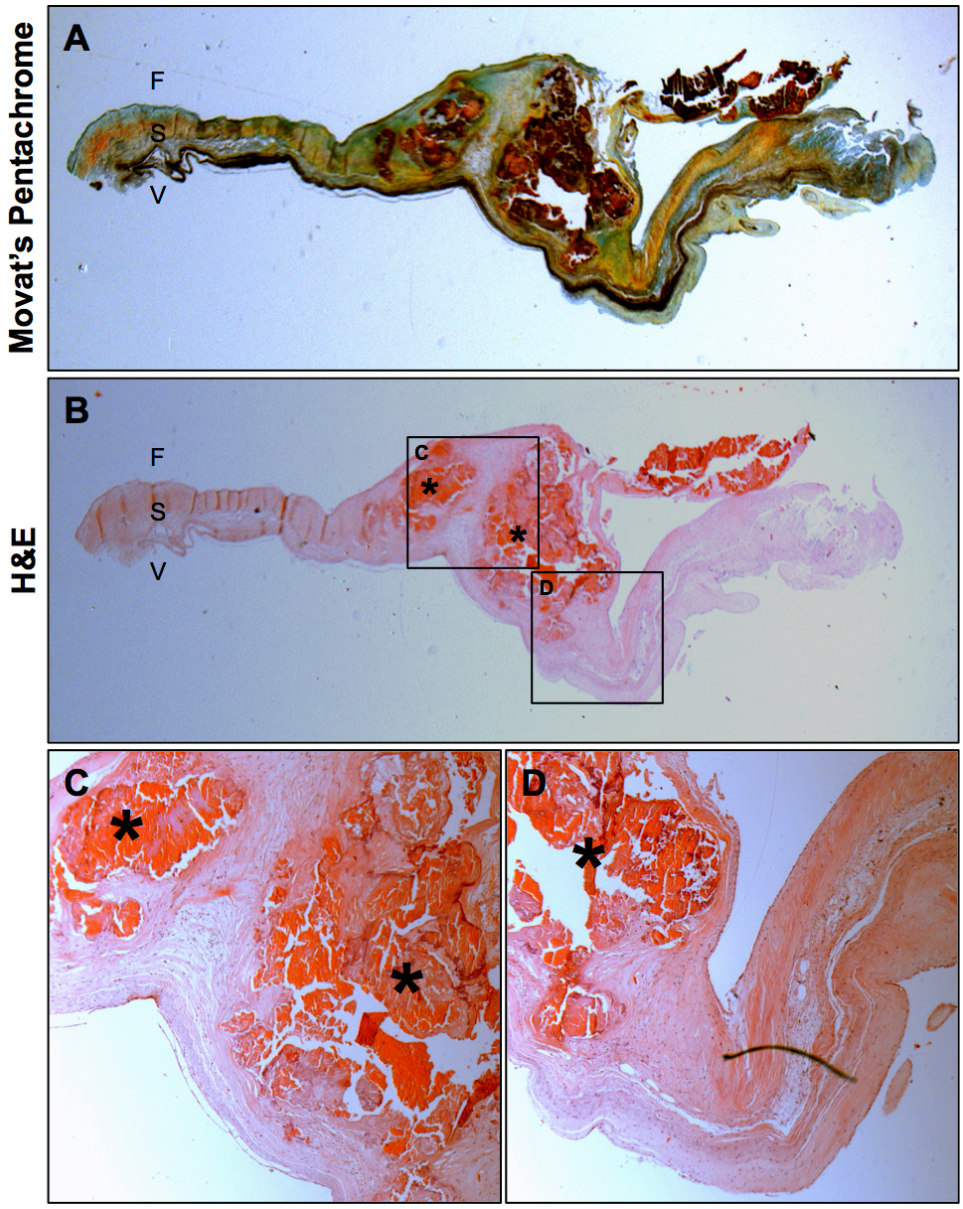

Figure SX. Movat's Pentachrome (**A**) and Hematoxylin and Eosin (H&E) stains (**B-D**) reveal dysregulated matrix, leaflet thickening, and severe calcification in calcified human aortic valves. Asterisks (*) indicate calcific nodules, F=Fibrosa, S=Spongiosa, V=Ventricularis.

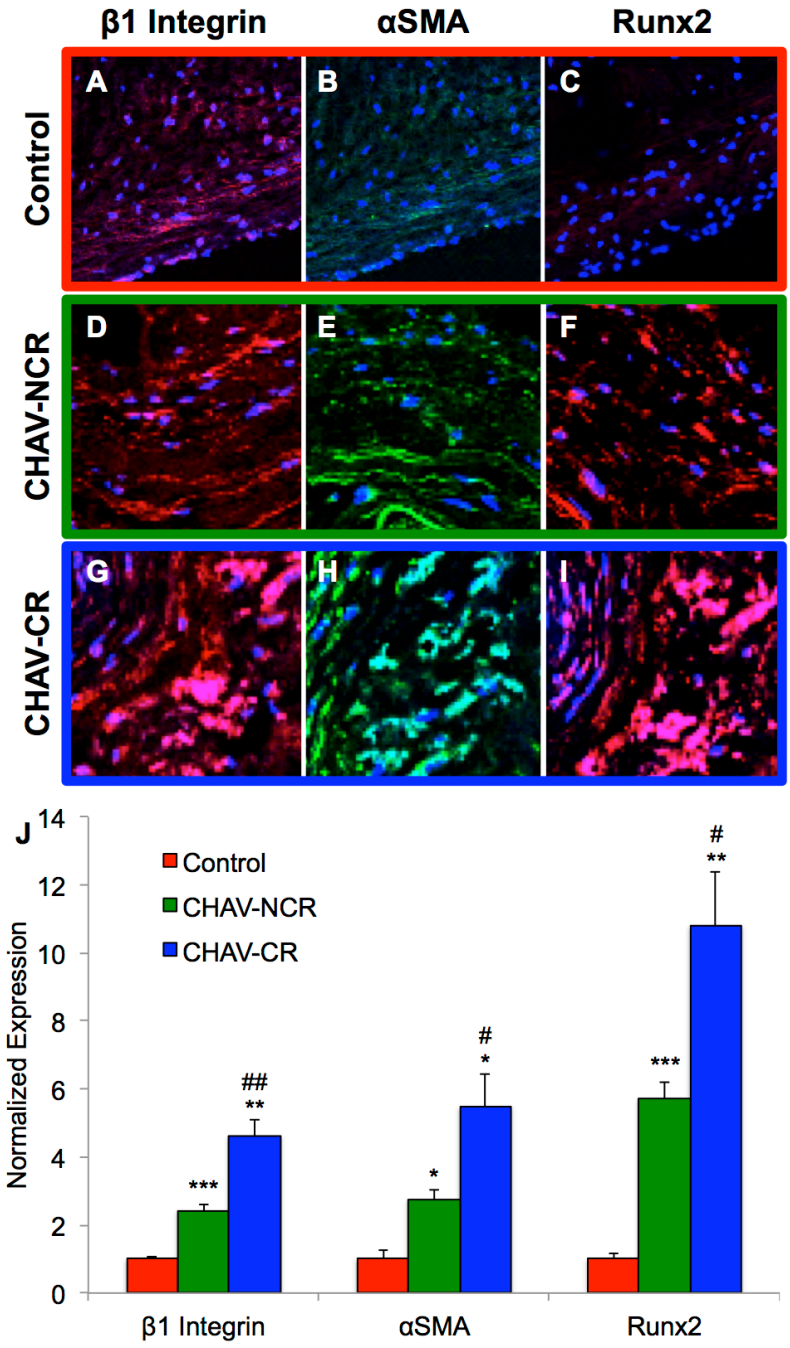

Figure SXI. β1 Integrin, αSMA, and Runx2 expression are lowest in control human valves (**A-C**) relative to calcified human aortic valves (CHAV). VICs in calcified regions (CR) of CHAV display increased expression of β1 Integrin, αSMA, and Runx2 (**G-I**) relative to non-calcified regions (NCR) of CHAV (**D-F**). Colored boxes correspond to magnified regions in **Figure 7**. CR=Calcified Region, NCR=Non-Calcified Region. Significance was determined using the Student's t-test (n=3 Control, n=5 CHAV, *p<0.01 **p<0.005 ***p<0.001 vs. Control, $^{\#}$p<0.05 $^{\#\#}$p<0.01 vs. CHAV-NCR)

	Nfatc1^{Cre}; *R26-Cad11*$^{Tg/Tg}$	*Nfatc1*^{Cre}; *R26-Cad11*$^{Tg/+}$	*Nfatc1*^{Cre}; *R26-Cad11*$^{+/+}$	p-value
Birth	22 (34.9%)	26 (41.3%)	15 (23.8%)	0.18
Expected	15.75 (25%)	31.5 (50%)	15.75 (25%)	

Table SI. Two *Nfatc1*^{Cre}*;R26-Cad11*$^{Tg/+}$ were mated and produced 6 litters, averaging 10.7 pups (total 63 pups). Pups were *Nfatc1*^{Cre}*;R26-Cad1*$^{Tg/Tg}$*, Nfatc1*^{Cre}*;R26-Cad11*$^{Tg/+}$*,* or *Nfatc1*^{Cre}*;R26-Cad11*$^{+/+}$. Chi-squared analysis using expected Mendelian ratios shows non-lethal effects of the Cad11 transgene (n=63, p=0.18)

Primer	Forward Sequence	Reverse Sequence
Pig 18s	AATGGGGTTCAACGGGTT	TAGAGGGACAAGTGGCGT
Pig Cad11	TGGAGATGGGATGGAATTGT	CTGATGAACTTCGGGTCGAT
Pig ACTA2 (αSMA)	CAGCCAGGATGTGTGAAGAA	TCACCCCCTGATGTCTAGGA
Pig RhoA	AACAGGATTGGTGCTTTTGG	CAGCAGGGTTCACAAGACA
Pig Sox9	GTACCCGCACCTGCACAAC	TCTCGCTCTCATTCAGCAGTC
Pig RunX2	GCACTACCCAGCCACCTTTA	TATGGAGTGCTGCTGGTCTG
Pig OCN	TCAACCCCGACTGCGACGAG	TTGGAGCAGCTGGGATGATGG

Table SII. Real-time PCR primers used for porcine genes.

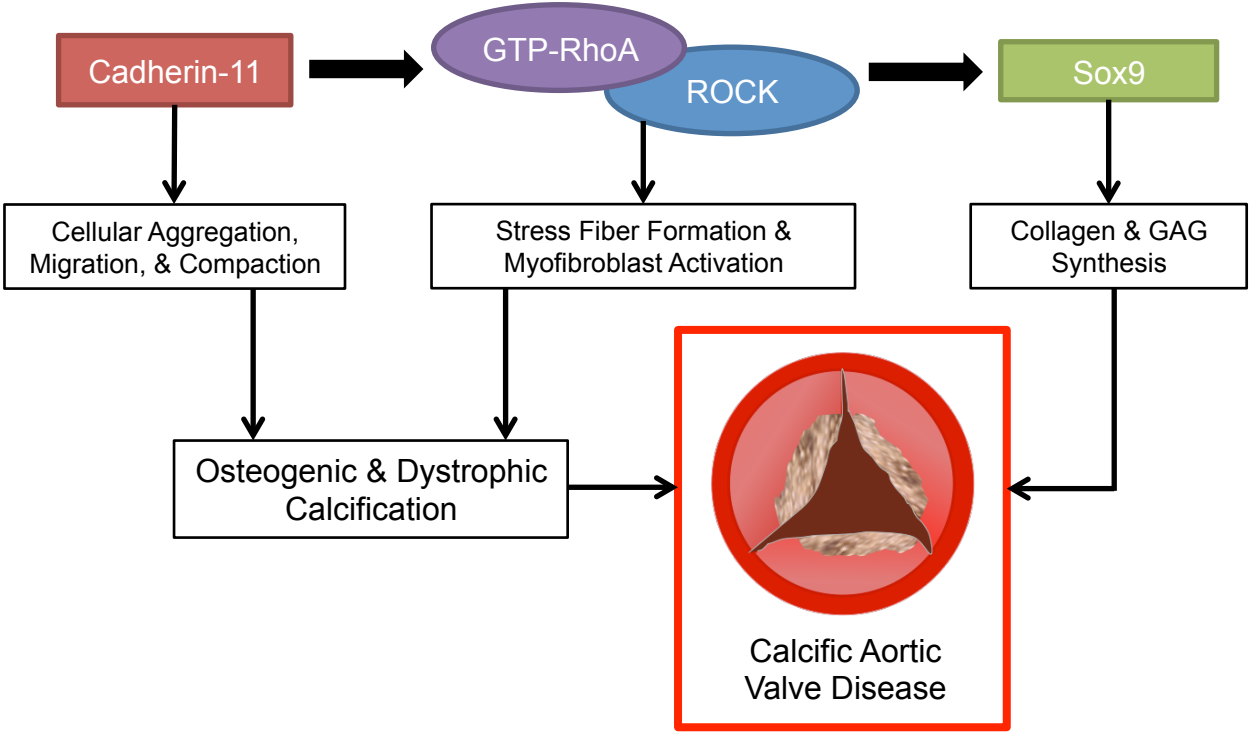
Cadherin-11
GTP-RhoA
ROCK
Sox9
Cellular Aggregation, Migration, & Compaction
Stress Fiber Formation & Myofibroblast Activation
Collagen & GAG Synthesis
Osteogenic & Dystrophic Calcification
Calcific Aortic Valve Disease